4
Effect of capsaicin coated silver nanoparticles on amyloid fibril formation of serum albumin

The process of amyloid formation of proteins is considered as one of the foundational events for the onset of a number of health problems (Aguzzi and O'Connor 2010b) (Greenwald and Riek 2010b). So far ~40 different amyloidogenic proteins are known to be associated with the onset of several neurodegenerative diseases (Greenwald and Riek 2010b)(Chiti and Dobson 2006b). Over the past decade, much research has been developed to surface functionalization of nanoparticles with selected compounds to target several biological processes including amyloid formation of proteins.

One of the most effective strategies to target amyloid-linked diseases is to find potential inhibitors against the initiation of the process of amyloid formation. In the previous chapter it was clearly evident that hydrophobic interactions play a critical role to initiate the aggregation process. Considering this assumption, it is possible that inhibitors, capable of interfering with the hydrophobic interactions between protein species, may act as inhibitors of the protein aggregation process. Hence, in this study, considering bovine serum albumin (BSA) as a model protein the effect of capsaicin as well as capsaicin coated silver nanoparticles ($AgNPs^{Cap}$) on amyloid formation of BSA has been studied. This work also synthesized control silver nanoparticles without capsaicin to test the significance of surface functionalization. Finally, molecular docking studies have been carried out to understand possible molecular interactions between capsaicin and BSA. The results provide a new approach to target aggregation of proteins by stable nanoparticles coated with aromatic natural compounds such as capsaicin.

4.1 EFFECT OF CAPSAICIN COATED NANOPARTICLES ON AMYLOID AGGREGATION.

In the past decades, many studies have focused on targeting inhibition of amyloid formation through various compounds such as natural products (Ghosh et al. 2009)(Kar and Kishore n.d.)(Shiraki et al. 2002)and selected peptides(Etienne et al. 2006)(Rajasekhar, Suresh, Manjithaya, Govindaraju, et al. 2015)(Viet et al. 2011b). Recent investigations have also looked at the effect of various nanoparticles on amyloid aggregation of proteins (Álvarez et al. 2013b)(Siposova et al. 2012b)(Dubey et al. 2015a)(Palmal, Jana, et al. 2014b). Some studies have suggested that nanoparticles coated with hydrophobic molecules are capable of inhibiting the fibrillation process of proteins (Siposova et al. 2012b)(Roberti et al. 2009)(Skaat et al. 2012b). It is also known that synthesized tyrosine and tryptophan coated nanoparticles not only suppress the amyloid formation of insulin but also trigger the disassembly of the mature amyloid fibrils (Dubey et al. 2014b).

Though capsaicin has gained much attention for its versatile medicinal properties, the effect of capsaicin on amyloid formation of proteins is largely unknown. Capsaicin is a well-known natural product that possesses multiple pharmacological properties including its anti-inflammatory (Frydas et al. n.d.), analgesic (Tandan et al. 1992)(Hempenstall et al. 2005) and ant tumorigenic (Huang et al. 2009)(Wutka et al. 2014) activities. Recent reports have also revealed the ability of capsaicin to bind to different proteins and to influence their functional properties (Perumal et al. 2015a) (Yang et al. 2015)(Zheng et al. 2015). Binding affinity of any molecule for the native as well as aggregation-prone intermediate structures of proteins is believed to be a

crucial factor for inhibition of protein aggregation. The capsaicin molecule appears to be an effective molecule to target aggregation-prone residues of an amyloidogenic protein due to its unique molecular structure comprising vanillyl, amide and aliphatic chain components. Reports on the effect of capsaicin and capsaicin coated nanoparticles on amyloid aggregation of proteins are scarce in literature.

4.1.1 Characterization of Capsaicin coated silver nanoparticles

Capsaicin coated silver nanoparticles $AgNPs^{Cap}$ were synthesized by following the established protocol (Amruthraj et al. 2015) (see materials and methods section). The formation of nanoparticles was confirmed by recording UV-visible absorption profiles of the sample. UV visible spectra of the sample containing $AgNPs^{Cap}$ nanoparticles showed typical SPR band at ~421 nm (Figure4.1B, red line)(Mulfinger et al. 2007). The obtained hydrodynamic radius of the nanoparticles using DLS is shown in Figure 4.1D, which reveals a diameter value that varies within ~10-40 nm. AFM data and transmission electron micrographs of $AgNPs^{Cap}$ samples are shown in Figure 4.1C and Figure 4.1E respectively. The obtained nanoparticles appeared spherical in shape displaying an average diameter value of ~50 nm. To understand the orientation of the surface functionalized capsaicin FTIR measurements were performed. Figure 4.1G shows FTIR signal of $AgNPs^{cap}$ nanoparticles where detected many characteristic bands were detected that appeared similar to the reported results on capsaicin coated silver nanoparticles (Amruthraj et al. 2015).

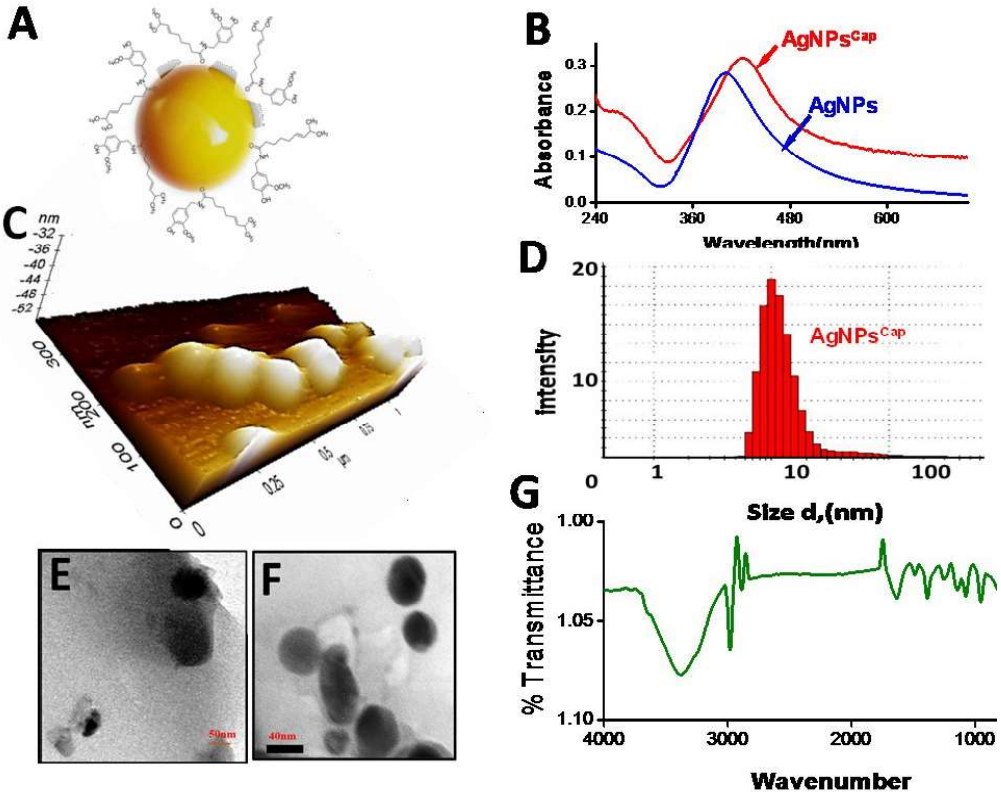

Figure 4.1: Characteristic properties of capsaicin coated silver nanoparticles. (**A**) Schematic representation of capsaicin coated silver nanoparticles ($AgNPs^{Cap}$). **(B)** UV-visible spectra of the capsaicin coated silver nanoparticle samples, $AgNPs^{Cap}$ (—) and control silver nanoparticles, AgNPs (—); **(C)** AFM topology image of $AgNPs^{Cap}$ nanoparticles. **(D)** Particles size distribution histograms of $AgNPs^{Cap}$ nanoparticles showing an average hydrodynamic radius of ~10-30nm. **(E)** TEM image of $AgNPs^{Cap}$ nanoparticles **(F)** TEM image of control AgNPs nanoparticles **(G)**FTIR data of the sample of $AgNPs^{Cap}$ nanoparticles which show the characteristic peaks

These data suggest that capsaicin molecules are functionalized to the surface of the nanoparticles through their C=O group as shown in the schematic diagram in Figure 4.1A. Further, the surface charge of the $AgNPs^{Cap}$ nanoparticles, as obtained from zeta potential measurements, was found to be -42 mV (Figure 4.2 C). These capsaicin capped nanoparticles were also observed to be very stable and the sample did not aggregate for a prolonged storage time at room temperature. In this study, control silver nanoparticles (without capsaicin, as mentioned in the methods section) were also synthesized, and the UV data of the control AgNPs (Figure 4.1B, blue curve) displayed a prominent peak at ~401 nm (Mulfinger et al. 2007). Size characterization of these nanoparticles were performed using DLS (Figure 4.2A) and visualized them using TEM (Figure 4.1F).

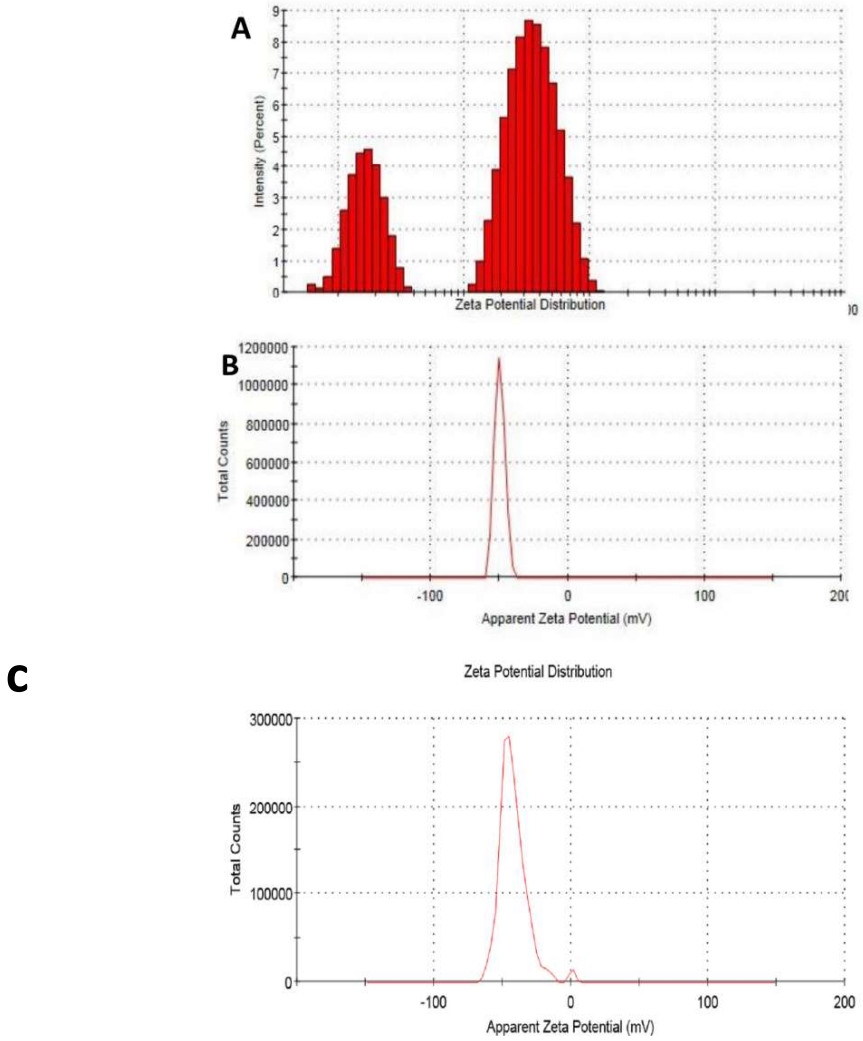

Figure 4.2: Characterization of size and zeta potential silver nanoparticles. (A) Particles size distribution histograms of AgNPs nanoparticles showing an average hydrodynamic radius of ~60nm. **(B)** The surface zeta potential graph for control silver nanoparticles showing a negative potential of -49.7 mV **(C)** The surface zeta potential graph for capsaicin capped silver nanoparticles showing a negative potential of -42 mV.

4.1.2 Effect of capsaicin coated silver nanoparticles on amyloid aggregation of BSA

Amyloid aggregation of BSA in PBS was studied at ~70°C (close to the T_m of BSA) (Dubey et al. 2014b)by monitoring the rise in the Thioflavin T signal at different time points. Monomers of BSA at ~5 μM showed a characteristic aggregation curve (Figure 4.3,⬟)

comprising of a distinct growth phase and a saturation phase. The nature of mature amyloid fibrils of BSA, as evident from AFM (Figure 4.5B) and TEM (Figure 4.5A) data, showed typical amyloid morphology as seen in the previous studies (Dubey et al. 2014b). The inhibition effect of capsaicin coated nanoparticles was examined at three different molar ratio values (of BSA: inhibitor) as mentioned in Figure 4.3. A gradual decrease in the ThT signals of the aggregating BSA sample with increasing concentrations of the $AgNPs^{Cap}$ nanoparticles was observed. This suggests a dose dependent inhibition of amyloid formation of BSA in the presence of $AgNPs^{Cap}$ nanoparticles (Figure 4.3).

To confirm this inhibition effect, as a next step, two control experiments were performed. First, the effect of isolated capsaicin molecules (at similar concentrations) on amyloid aggregation of BSA was studied and the results are shown in figure 4.3 (●) and (▲). Second, the effect of control AgNPs (uncoated, without capsaicin) on the aggregation process of BSA

(Figure 4.3▼). Obtained results from both the control experiments prove that only capsaicin coated $AgNPs^{Cap}$ nanoparticles are capable of showing anti-amyloid property (Figure 4.3A: ◆,◀,▶).

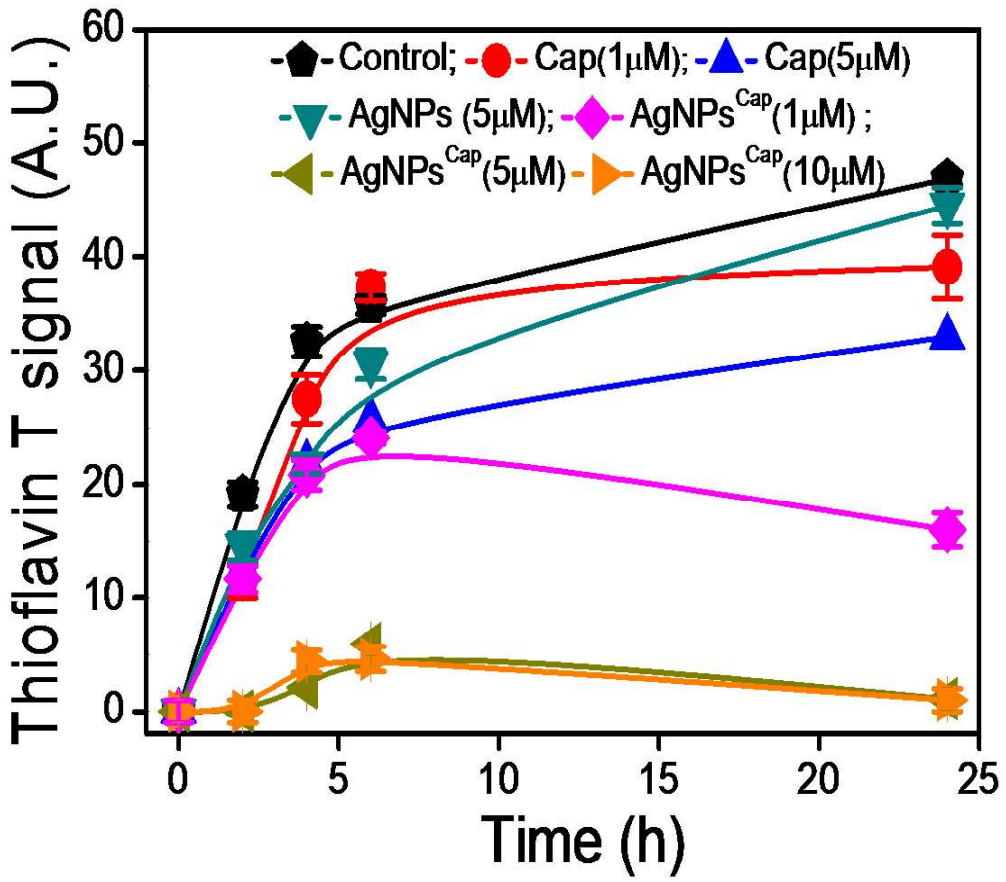

Figure 4.3: Effect of capsaicin, AgNPs and $AgNPs^{Cap}$ on aggregation of BSA. ~5 μM BSA sample at different molar ratios was used: (⬟) 5μM BSA only; (●) 5μM BSA + 1μM capsaicin; (▲) 5μM BSA + 5μM capsaicin; (▼) 5μM BSA + 5μM control AgNPs; (◆) 5μM BSA + 1μM $AgNPs^{Cap}$; (◀)5μM BSA + 5μM $AgNPs^{Cap}$; (▶) 5μM BSA + 10μM $AgNPs^{Cap}$.

However, at higher concentrations isolated capsaicin molecules did show slight inhibition effect on amyloid aggregation of BSA (Figure 4.4). This result confirms that capsaicin molecules are highly effective in inhibiting the formation of amyloid fibrils only when they are attached to the surface of the nanoparticles. Similar observation on the importance of surface

functionalization of nanoparticles to achieve inhibition of protein aggregation has been recently reported (Dubey et al. 2015a). Notably, these AgNPs^{Cap} nanoparticles can be considered as strong inhibitors of BSA because complete suppression of the aggregation process was observed even at 1:1 molar ratio value of protein: inhibitor.

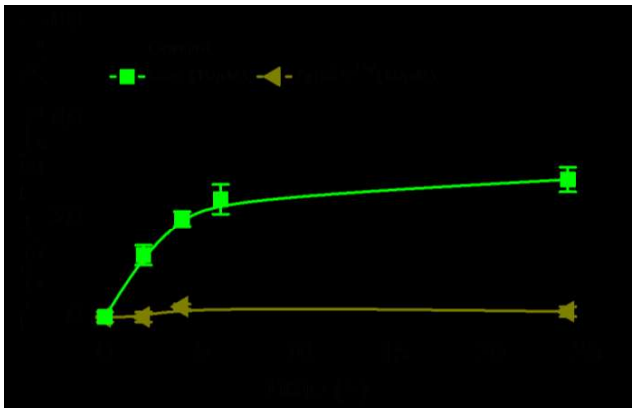

Figure 4.4: Effect of capsaicin and AgNPs^{Cap} at high concentration on the aggregation process of BSA. Black line denotes the kinetic curve for the control BSA; green curve indicates the aggregation of BSA+Capsaicin at 10μM. olive curve indicates the aggregation of BSA+ AgNPs^{Cap} at 10μM.

Next, the secondary structure contents of the mature amyloid fibrils of BSA taken from an inhibited reaction in the presence of AgNPs^{Cap} were studied using FTIR methods. The second derivative FTIR data, as shown in Figure 4.5C, reveal several characteristic peaks (1616 cm^{-1}, 1635 cm^{-1}, 1646 cm^{-1}, 1667 cm^{-1} and 1684 cm^{-1}), particularly suggesting the prevalence of intermolecular β-sheets as reported for BSA (Lu et al. 2015). This result suggests that AgNPs^{Cap} nanoparticles may be delaying the formation amyloid fibril without altering the aggregation pathway.

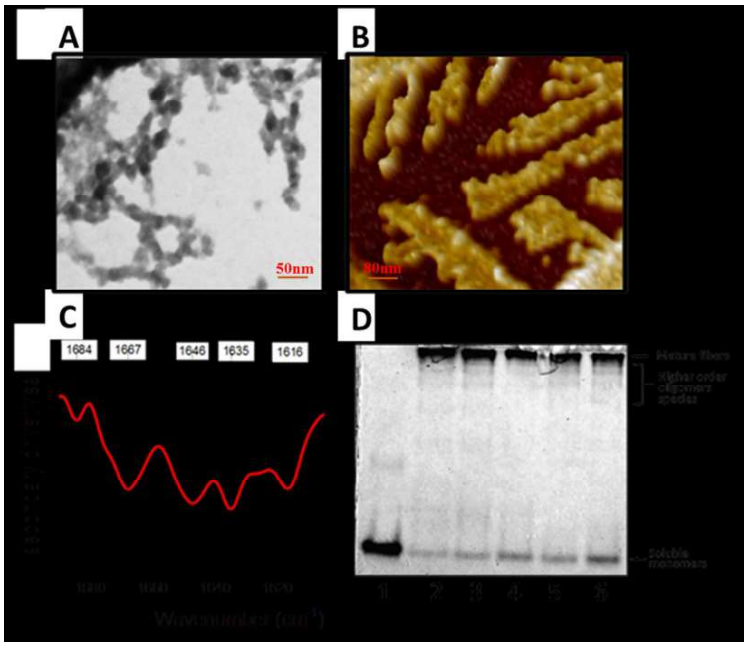

Figure 4.5: Structural properties of BSA amyloid fibers: (A) TEM image of negatively stained mature BSA amyloid fibrils. (**B**) AFM image of mature BSA**(C)** ATR-FTIR second derivative spectra of inhibited BSA amyloid fibers in presence of capsaicin coated silver nanoparticles. Molar ratio of protein: inhibitor was kept at 1:1. **(D)** Native gel-electrophoresis of the BSA (~5 μM) sample under aggregating conditions at 6h time point. (1) Control soluble BSA; (2) BSA aggregates without inhibitors (~5 μM); (3) BSA + capsaicin (~5 μM); (4) BSA + capsaicin coated nanoparticles (~1 μM) (5) BSA + capsaicin coated nanoparticles (~5 μM) (6) BSA + capsaicin coated nanoparticles (~10 μM).

4.1.3 Molecular interaction of capsaicin with BSA

Next, molecular docking studies on BSA-Capsaicin interactions were carried out to further understand the observed inhibition effect. Blind docking studies (see methods section) predicted a viable capsaicin-BSA interaction at a site within BSA's A-chain which spans from Tyr 400 – Leu 582. The value of CDocker energy for the best pose as shown in Figure 4.6 was -31.2 kcal.mol^{-1} and its corresponding interaction energy was observed to be -35.3 kcal.mol^{-1}.

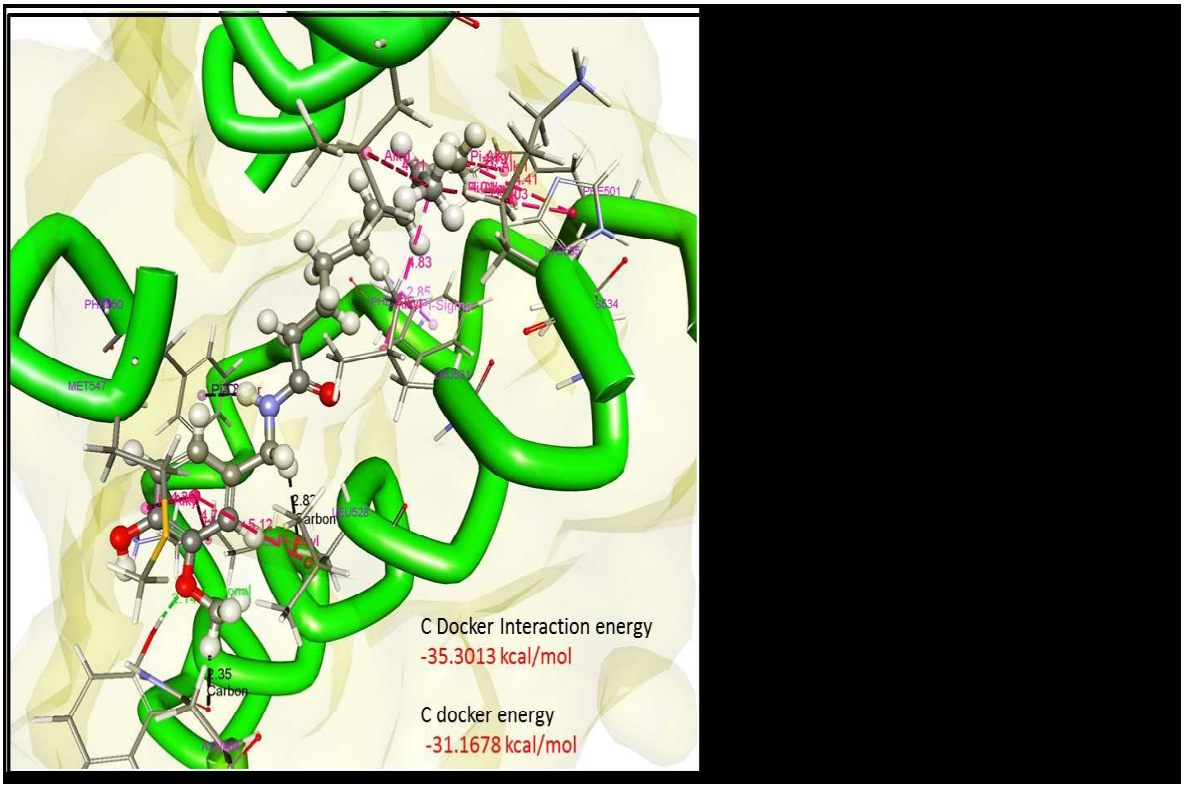

Figure 4.6: Molecular docking studies of a capsaicin molecule with BSA: The BSA-capsaicin complex shows fourteen possible interactions comprising of one hydrogen bond two carbon bonds one pi-sigma pi-donor two alkyl and seven pi-alkyl bonds. Right panel of the figure lists all the interactions between capsaicin and BSA.

Such energy values predict the formation of a stable protein-ligand complex. Capsaicin-BSA complex structure displays fourteen interactions as listed in the right panel of the Figure 4.6. Notably, the docking studies have predicted five strong interactions (TYR400:CapsaicinO2, ASN401:CapsaicinH49, LYS524:CapsaicinH34, PHE506:CapsaicinH27and PHE550: CapsaicinH36) which mostly involve hydrophobic and electrostatic interactions. To identify the critical residues in the BSA sequence (PDB ID: 4F5S) which are predicted to promote amyloid aggregation, online tools PASTA 2.0 (Walsh et al. 2014) and AGRESCAN3D (Zambrano et al. 2015) were employed and the obtained data are shown in Figure 4.7-4.9 and Table 4.1. The aggregation propensity and the degree of disorderness data as shown in figure 4.7A and 4.7B reveal that the region spanning from Tyr400 to Leu582 is the aggregation prone tract of BSA. This prediction is further supported by the information obtained from AGGRESCAN3D (Table 4.1, Figure 4.8 and 4.9). Interestingly, most of the amino acids that interact with capsaicin (from Figure4.6) are from the predicted aggregation prone regions of BSA (Figure 4.8 and 4.9).

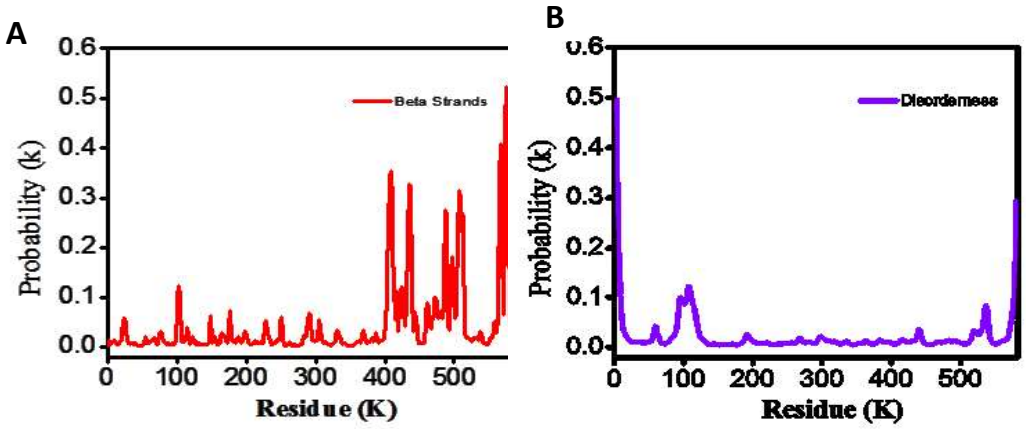

Figure 4.7: Sequence analysis of BSA using PASTA. (A) Probability of beta structures in BSA sequence. (B) Disorderness profile of amino acid residues of the BSA protein. The PDB ID of BSA considered for this study is 4F5S. The analysis of sequence was performed using the available online tool, PASTA 2.0

Table 4.1: AGGRESCAN 3D score for the aggregation prone amino acid residues in BSA (based on the A3D scoring values). The red stars indicate the residues that interact with capsaicin as evident from the molecular docking studies.

Amino acid residue index	Amino acid residue	Chain	Aggrescan 3D score
576	V	A	1.1452
569	V	A	0.6943
551	V	A	0.5666
575	V	A	0.3228
579	Q	A	0.2579
580 ★	T	A	0.2234
577	S	A	0.1345
578	T	A	0.0329
538	A	A	0.0000
557	C	A	0.0000
553	F	A	0.0000
567	F	A	0.0000
512	I	A	0.0000
533	K	A	0.0000
528	L	A	0.0000
531	L	A	0.0000
532	L	A	0.0000
543	L	A	0.0000
525	Q	A	0.0000
529	V	A	0.0000
546	V	A	0.0000

Amino acid residue index	Amino acid residue	Chain	Aggrescan 3D score
569	V	B	0.9661
576	V	B	0.8174
551	V	B	0.2140
538	A	B	0.0000
513	C	B	0.0000
557	C	B	0.0000
530	E	B	0.0000
550 ★	F	B	0.0000
553	F	B	0.0000
567	F	B	0.0000
512	I	B	0.0000
533	K	B	0.0000
528 ★	L	B	0.0000
531 ★	L	B	0.0000
532	L	B	0.0000
543	L	B	0.0000
525	Q	B	0.0000
529	V	B	0.0000

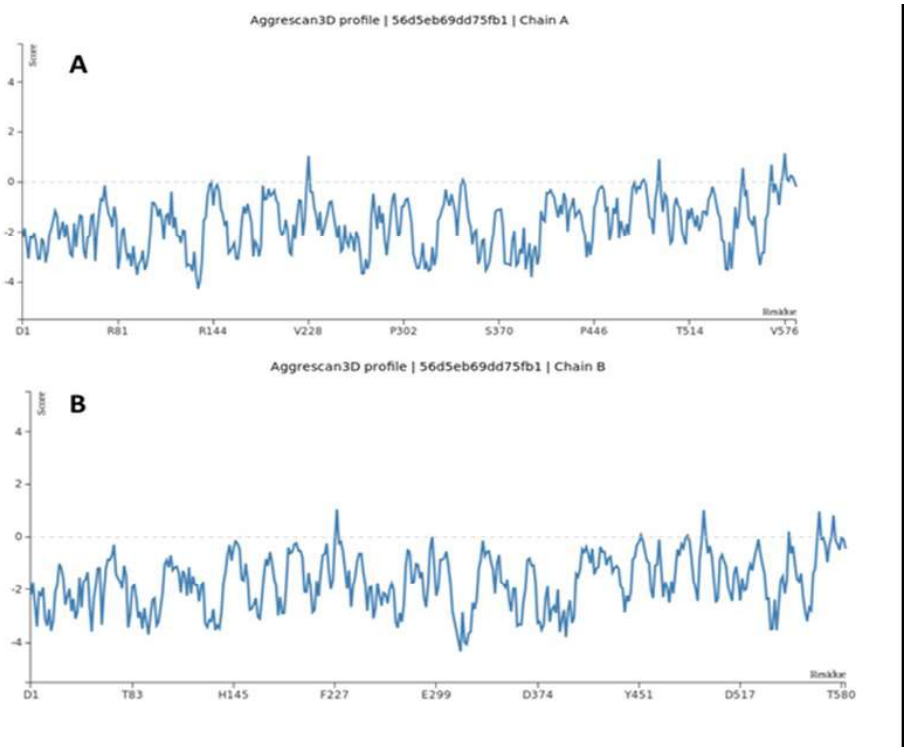

Figure4.8: Prediction of aggregation prone regions by AGGRESCAN 3D online tool. AGGRESCAN 3D plot showing the aggregation propensity of the residues in the A-chain (panel A) and B-chain (panel B) of BSA protein (PDB ID 4F5S). Here, the X-axis represents amino acids and Y-axis represents their respective A3D scores. The residual score above 0 are considered as aggregation prone. The residual score below 0 are meant to be soluble residues.

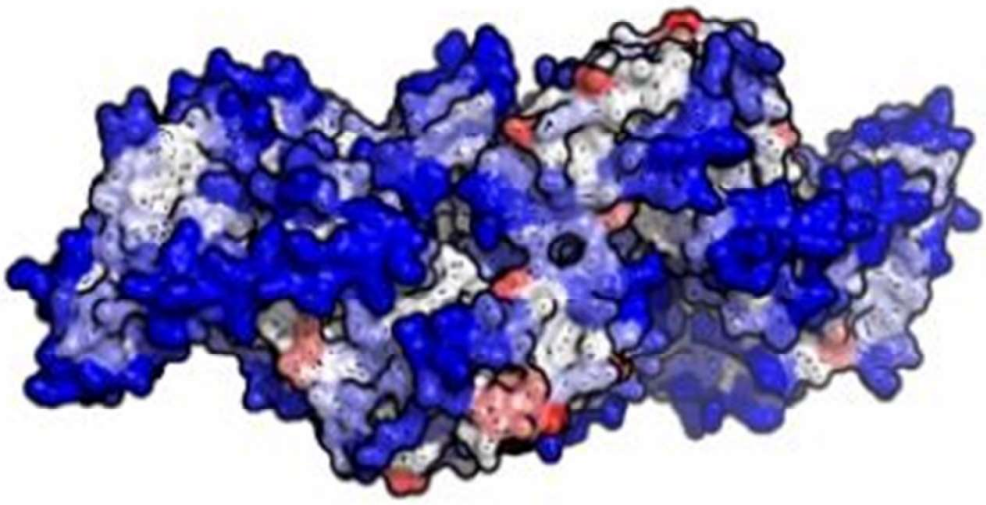

Figure4.9: Snapshot of aggregation prone regions by AGGRESCAN 3D. The protein surface is colored according to A3D score in gradient from red (high-predicted aggregation propensity) to white (negligible impact on protein aggregation) to blue (high-predicted solubility).

4.2 DISCUSSION

This work clearly reveals the potential of the capsaicin coated silver nanoparticles ($AgNPs^{Cap}$) to inhibit amyloid fibril formation of BSA. Obtained results confirm that surface functionalization of capsaicin molecule is vital for its inhibitory effect against amyloid formation because such inhibition effect was not observed in the presence of isolated capsaicin molecules as well as control uncapped nanoparticles. It has been suggested that structural constraints and specific aromatic interactions are two key factors to facilitate the interaction between the inhibitor and the amyloidogenic core of the protein(Gemma Soldi et al. 2006). It is much likely that surface functionalization would preferably allow the functional groups of the capsaicin molecules to participate in crucial interactions with the corresponding reactive groups of the protein molecule at the site of binding.

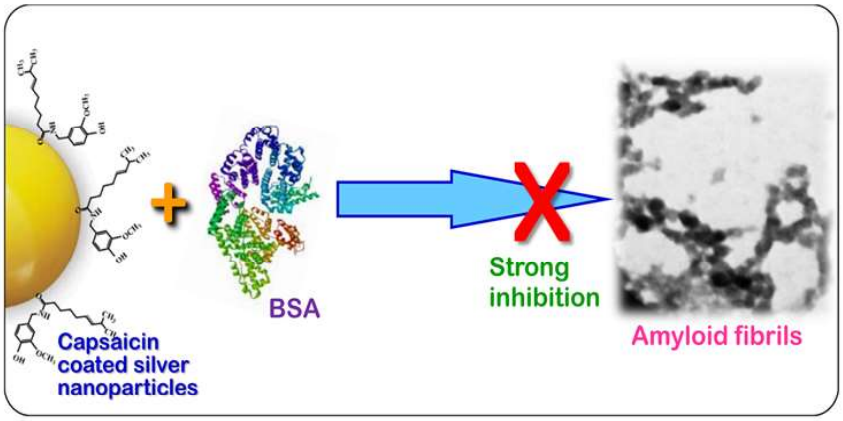

Figure4.10: Schematic representation of BSA amyloid inhibition by Capsaicin coated silver nanoparticles.

FTIR data suggest the functionalization of capsaicin molecule on the nanoparticles though C=O group and such orientation of attached capsaicin would presumably allow its vanillyl group, amide group and the aliphatic tail region to enhance capsaicin's binding affinity for proteins (Yang et al. 2015). The stabilization of the native conformation of proteins due to ligand binding is believed to be an important factor for prevention of amyloid aggregation of proteins (Gemma Soldi et al. 2006). The molecular docking studies and bioinformatics analysis predict capsaicin's ability to participate in H-bond, CH-π and electrostatic interactions with the key aggregation-prone residues of BSA (Figure 4.6). Temperature induced amyloid formation process of BSA is believed to be mediated by intermolecular association between partially folded intermediate species with exposed hydrophobic residues. If the ligand molecule is capable of interfering with the intermolecular association of aggregation prone species, it may eventually prevent the process of protein aggregation. Additionally, stabilization of native conformation would also reduce the population of aggregation prone intermediate species during the process of temperature induced amyloid fibril formation. In this work, it was found that the native conformation of BSA is retained under aggregating condition in the presence of $AgNPs^{Cap}$ nanoparticles (Figure4.5D). Recently, it was reported that negatively charged hydrophobic nanoparticles can prevent Aβ amyloid fibril formation by interfering with the hydrophobic and electrostatic interactions (Liu et al. 2016). Here, the $AgNPs^{Cap}$ nanoparticles were found to possess a negative potential of -42mV (Figure 4.2C) and with such a value of negative potential the nanoparticles are predicted to influence the electrostatic interaction between protein and the ligand, suppressing the inherent aggregation-propensity of the protein species. Here, it is much likely that through surface functionalization of capsaicin molecule the reactivity of its vanillyl and the aliphatic chain components towards the aggregation-prone hydrophobic residues of BSA is enhanced.

4.3. CONCLUSION

This chapter reveals capsaicin's anti-amyloid activity when it is surface functionalized with silver nanoparticles. Bioinformatics analysis reveals CH-π and H-bonding interactions between capsaicin and BSA in the formation of protein-ligand complex. These results suggest the significance of surface functionalization of nanoparticles with capsaicin which probably enables capsaicin to effectively interact with the key residues of the amyloidogenic core of BSA. Since complete inhibition of amyloid fibril formation was observed at 1:1 molar ratio of $AgNPs^{Cap}$: BSA. However, isolated capsaicin and uncapped control nanoparticles did not show such inhibition effect. These amyloid inhibitors are highly relevant for future designing of therapeutics against amyloid-linked diseases.

...